Formation, Structure, and Rheological Properties of Ricinelaidic Acid–Vegetable Oil Organogels

Amanda J. Wright[a,*] and Alejandro G. Marangoni[b]

[a]Department of Human Health and Nutritional Sciences, College of Biological Sciences, and
[b]Department of Food Science, Ontario Agricultural College, University of Guelph, Guelph, Ontario Canada, N1G 2W1

ABSTRACT: Vegetable oil-based organogels were formed using ricinelaidic acid (12-hydroxy-9-*trans*-octadecenoic acid, REA). Gelation kinetics, gel structure, and stability were studied. Gelation occurred with as little as 0.5% (w/w) REA, depending on temperature and oil composition. Phase diagrams were constructed using canola, sesame, and DAG oils. Lower gelation tendencies were correlated with the presence of potential hydrogen-bonding moieties in the oils. REA concentration had a significant influence on gelation kinetics and gel rheology. At 5°C, the 0.5% canola oil gel behaved like a weak, viscoelastic network composed of entangled strands. Between 1.0 and 5.0% REA, solid-like, viscoelastic gels were formed. The 24-hour G'_{LVR} (storage modulus in the linear viscoelastic region) was highly dependent on concentration and less so on temperature. Values for gelation time indicated a change in behavior below 2% REA and above 20°C. Polarized light microscopy revealed that the gels were formed through the interactions of long, thin, and birefringent fibers. Structural analysis using X-ray diffractometry (XRD) indicated the presence of repeating REA dimers and increasing order with concentration and gel storage time. Increases in gel opacity, birefringence, XRD scattering, and fiber clustering were observed during storage.

Paper no. J11277 in *JAOCS 83*, 497–503 (June 2006).

KEY WORDS: Gelation, nanofibers, organogels, phase behavior, rheological properties, ricinelaidic acid, self-assembly.

Organogels constitute a diverse group of gelled materials in which the immobilized liquid is nonaqueous. The ability of these materials to self-assemble on the nanoscale and to solubilize lipophilic guest molecules makes them useful in purification and separation processes, as media for nonaqueous synthesis or reactions, and in drug delivery. In addition, the sharp temperature and moisture sensitivities of many organogels make them useful in sensing and controlled release scenarios. Uses of organogels include environmental cleanup, safe transport of flammable liquids, aerogel formation, ingredients in lubricants and coatings, and in pharmaceutical and food technologies (1–3).

Although the term "organogel" refers most typically to a completely nonaqueous system, some largely organic systems that gel only in the presence of small amounts of water are also referred to as organogels. For example, when small amounts of water are added to organic solutions of lecithin, gelation occurs (4). This type of gelled microemulsion has been termed an organogel. Organic liquids also can be immobilized through the *in situ* formation of covalent bonds between network molecules (5). These so-called chemical gels have interesting applications, but only those organogels that form through physical associations will be considered here.

Organogels are viscoelastic and thermally reversible. They form through the self-assembly of gelator molecules at low concentrations (often <1%). The aggregated molecules form superstructures, often long fibers, which entangle or form pseudo-crystalline regions, immobilizing the liquid largely by surface tension and forming a gel of variable consistency (2,3). The networks that form are reminiscent of macromolecular gels and polymers. However, their thermoreversibility and nucleation involving one-dimensional crystal growth distinguish organogels from materials such as cross-linked polystyrene (6).

Organogelators have relatively low M.W. compared with those molecules that form the gel networks in typical hydrogels. Some organogelators include derivatives and metal salts of FA (7,8) and steroids (6), amino acid-type molecules (9,10), carbohydrate amphiphiles (11), and organometallic compounds (12,13). These molecules are amphiphilic in nature and self-assemble in hydrophobic liquids when an appropriate balance between the solubility and aggregation forces exists (2). Aggregation occurs primarily through dipolar interactions, specific intermolecular hydrogen bonding, and metal coordination bonding (2). The nature of both the solvent and gelator influences gel formation and morphology (14). Although a considerable amount of effort has gone into identifying suitable gelator–solvent combinations, there is still much to learn in this regard (2).

Organogelation could serve useful functions in foods and nutraceuticals (15). It would be beneficial, for example, to structure liquid oils without hypercholesterolemic saturated or *trans* FA or to minimize oil migration in composite food products. The possibility of using organogels to stabilize nutraceuticals and enhance their delivery is also intriguing. Our long-term objective is to identify organogelators with food or nutraceutical potential using the structures of known gelators as templates. Hydroxystearic acid (HSA, 12-hydroxy octadecanoic acid), is a well-known gelator of organic liquids and is commonly used in cosmetics as well as lubricating greases and coatings (14,16). The hydroxylated FA is formed through the hydrogenation of castor oil, a material rich in ricinoleic acid

*To whom correspondence should be addressed.
E-mail: ajwright@uoguelph.ca

(12-hydroxy, 9-octadecenoic acid). HSA organogel research has served as a model for further exploration of organogels (2). The purpose of this study was to explore the ability of ricinelaidic acid (REA; 12-hydroxy, 9-*trans*-octadecenoic acid) to gel vegetable oil and to characterize the gelation behavior and gel structure.

EXPERIMENTAL PROCEDURES

Materials and sample preparation. REA (>99% purity; Nu-Chek-Prep, Elysian, MN) was blended with refined, bleached, and deodorized (RBD) canola oil (CO; Bunge, Toronto, Canada) at 0.1–5.0 wt% levels. The samples were heated to 80°C, mixed vigorously, and held at 80°C for 10 min before subsequent experiments. The melting temperature of REA was determined by differential scanning calorimetry (DSC) using a Q-1000 calorimeter (TA Instruments–Waters LLC, New Castle, DE). Samples (8–10 mg) were hermetically sealed in aluminum pans, crystallized at 5°C for 24 h, and then heated at a rate of 5°C/min. Peak melting temperatures were determined using the software provided with the instrument.

Gelation behavior. Phase diagrams were constructed using the blends of REA and CO just mentioned. Vials containing 1 mL of the blends were held at temperatures between-10 and 50°C. After 24 h, the vials were inverted and the self-standing ability of the samples was assessed visually. Depending on appearance, samples were described as liquid, thickened liquid, clear gel, translucent-opaque gel, or fat-like. To evaluate the influence of oil composition on gelation, phase diagrams were also constructed for REA with unrefined sesame seed (Sunfresh Ltd., Toronto, Canada) and DAG (Enova, ADM Kao LLC, Decatur, IL) oils.

Gelation of the 0.5, 1.0, and 5.0% REA–CO samples at 5°C was also monitored by small-deformation rheology using an AR 2000 rheometer (TA Instruments, Mississauga, Ontario, Canada). Oscillatory stress sweeps (0.15% strain and 1 Hz) were performed periodically (every 14 min) after loading the samples at 80°C into a temperature-controlled aluminum recessed-end concentric cylinder at 5°C (1 mm spacing between cylinders and 2000 μm gap).

Gel structure and rheological properties. Gel structure was visualized by bright-field and polarized light microscopy using an Olympus BH microscope (Olympus, Tokyo, Japan). Small samples (~15 mg) of the gels were placed on glass microscope slides and gently covered with glass coverslips. Slide temperature was maintained using a Linkam LTS350 cold stage (Linkam Scientific Instruments Inc., Surrey, England). Digital images of the partially and fully polarized specimens were acquired using a Sony XC75 CCD camera and LG-3 capture board (Scion Corporation, Frederick, MD).

Gel structure was also studied using a Rigaku MultiFlex X-Ray Diffractometer (The Woodlands, TX). Glass holders with sample wells (0.5mm depression) were loaded with hot samples and held for 1, 7, 14, and 28 d at 5°C. Sample temperature during analysis was maintained by placing a Peltier plate at 5°C directly beneath the sample holder. Angular scans were performed at 0.5° per minute from 1 to 30° 2θ using a Cu source X-ray tube at 40 kV and 44 mA. Background subtractions to remove liquid oil scattering and peak detection/labeling were performed using the Jade 6.5 software (Materials Data Incorporated, Livermore, CA).

Characteristic small-deformation dynamic rheological parameters of the gels were determined after 1, 7, 14, and 28 d at temperatures between 5 and 30°C. Three milliliters of each sample was placed in a 4-mL vial at the desired temperature and loaded onto the flat plate of the AR2000 rheometer (TA Instruments, New Castle, DE) after the specified times, and storage moduli (G') in the linear viscoelastic region (LVR) were determined. A 6 cm, 2° acrylic cone with truncation gap of 66 μm was used. Strain sweeps were performed from 6.0×10^{-3} to 2.0% at a frequency of 1 Hz. Frequency sweeps from 0.1 to 10 Hz were also performed after 24 h at 5°C using a controlled strain of 0.1%.

RESULTS AND DISCUSSION

Gelation and phase behavior. REA was found to gel CO, depending on concentration and temperature. Gelation times for the REA-CO blends are shown in Table 1.

The concentration dependence of REA gelation is evident. Even after several months at 5°C, no gelation was observed below 0.5% REA. At 0.5% a gel was observed after 20.5 h. With 1% REA, t_{gel} decreased dramatically to roughly 11 min. With increasing concentration, an exponential decrease in t_{gel} was observed at 5°C. At each temperature studied, concentration had a significant influence on t_{gel} ($P < 0.05$). However, for each concentration above 1%, significantly higher values of t_{gel} were not observed until above 20°C. For concentrations of 2% and above, t_{gel} was independent of temperature, up to 20°C. Above 20°C, a dramatic increase in t_{gel} was observed for the gels, indicating the existence of a different gelation regime.

Gelation behavior at 5°C was also monitored by small-deformation rheology. Figure 1A shows the changes in the storage modulus (G') during gelation of the 0.5, 1.0, and 5.0% REA blends at 5°C.

With 1.0 and 5.0% REA, gelation occurred very rapidly at 5°C. The samples quickly reached a maximum in G', ~24,000 and ~65,000 Pa, respectively. Such sharp sol-to-gel transitions are characteristic of "strong" organogels, which demonstrate solid-like viscoelastic behavior (2). In contrast, the most dilute sample (0.5%) gelled gradually in a manner more typical of "weak" gel-like systems, which possess liquid-like viscoelastic properties (2). An increase in G' was observed throughout the duration of the experiment, reaching a value of ~370 Pa after 68 h. Characteristic viscoelastic parameters of the REA-CO gels after 24 h were determined. Figure 1B shows that concentration had a significant effect on gel strength ($P < 0.05$).

The 24-h phase diagram for REA with CO (REA-CO) is shown in Figure 2A. Four phases were identified according to the visual appearance of the samples. These were A: fat-like (i.e., the material appeared more polycrystalline than gel-like), B: translucent-opaque gel (i.e., self-standing gels ranged from

TABLE 1
Gelation Time[a] (t_{gel}, s)[b] for 0.5, 1.0, 2.0, 3.0, 4.0, and 5.0% REA–Canola Oil Blends Between 5 and 40°C

Temperature (°C)	0.5%	1.0%	2.0%	3.0%	4.0%	5.0%
5	7.4025 ± 4512	660 ± 91[a]	446 ± 12[a]	341 ± 6[a]	290 ± 38[a]	207 ± 59[a]
10	NG	886 ± 80[b]	458 ± 49[a]	326 ± 41[a]	306 ± 36[a]	265 ± 35[a]
15	NG	3359 ± 993[c]	353 ± 5[a]	227 ± 4[b]	187 ± 6[a]	145 ± 8[a]
20	NG	NG	517 ± 24[a]	342 ± 4[a]	224 ± 27[a]	190 ± 6[a]
25	NG	NG	1819 ± 28[b]	1693± 46[c]	1136 ± 240[b]	795 ± 75[b]
30	NG	NG	NG	NG	2959 ± 475[c]	1638 ± 125[c]
35	NG	NG	NG	NG	NG	NG
40	NG	NG	NG	NG	NG	NG

[a]Mean ± SD (n = 6). Within each column, different superscripts (a–c) indicate a significant difference ($P < 0.05$).
[b]Time when material is self-standing in inverted vial. REA, ricinelaidic acid; NG, no gelation after 24 h.

slightly translucent to completely opaque), C: clear gel (i.e., self-standing gel was completely transparent), and D: liquid (i.e., no thickening or gelation was observed).

The minimum REA concentration at which gelation occurred was 0.5%. A clear gel formed at this concentration at 5°C, but not at 10°C. According to Figure 2A, the concentration and temperature range at which a clear gel formed was very narrow. By 1%, the gels were slightly cloudy. With increasing REA content, increased opacity was observed. By 3.5%, the samples were gelled, but opaque. Gel appearance depended more on concentration than temperature; within each concentration, sample opacity was similar across the temperature range at which setting occurred. Larger changes in the appearance of the samples were observed with increasing temperature. Similarly, there was no transition region in the upper temperature range for gelation. For example, a clear gel was not observed for the 2% sample around 25°C, nor was an opaque gel observed for the 4% sample around 40°C.

The peak melting temperature of pure REA was 50.3 ± 0.1°C, whereas the maximum gelation temperature was 30°C with 5% REA. Maximum gelation temperatures generally do not correspond to the melting temperatures of the neat gelators (2). According to the van't Hoff equation, some of the REA will be solubilized in the oil phase, thereby lowering the melting temperature of the gels vs. pure REA. Even above the solubility limit, gelation will be dependent on having a threshold REA concentration that results in enough organized molecules to form a space-filling network capable of entrapping CO. Also, based on the similarities of REA to HSA, hydrogen bonding is expected to play a critical role in the aggregation of REA molecules into the long network strands. Hydrogen bonding between hydroxyl groups causes HSA aggregation in organic solvents (8). Since the strength of hydrogen bonding decreases with increasing temperature, this also may partially limit REA aggregation at higher temperatures.

Solvent nature, polarity, and the presence of cosurfactants can influence the aggregation of organogelator molecules (2). To investigate the influence of solvent on REA gelation, phase diagrams were constructed using unrefined sesame oil and DAG oil. The phase diagram for REA with sesame oil is shown in Figure 2B. Comparison of Figures 2A and 2B shows that the upper limits for REA gelation were lower with sesame oil than with CO. Unrefined sesame oil is characterized by relatively higher levels of free FA, sterols, and tocopherols than RBD CO (17). Each of these compounds contains hydroxyl groups with

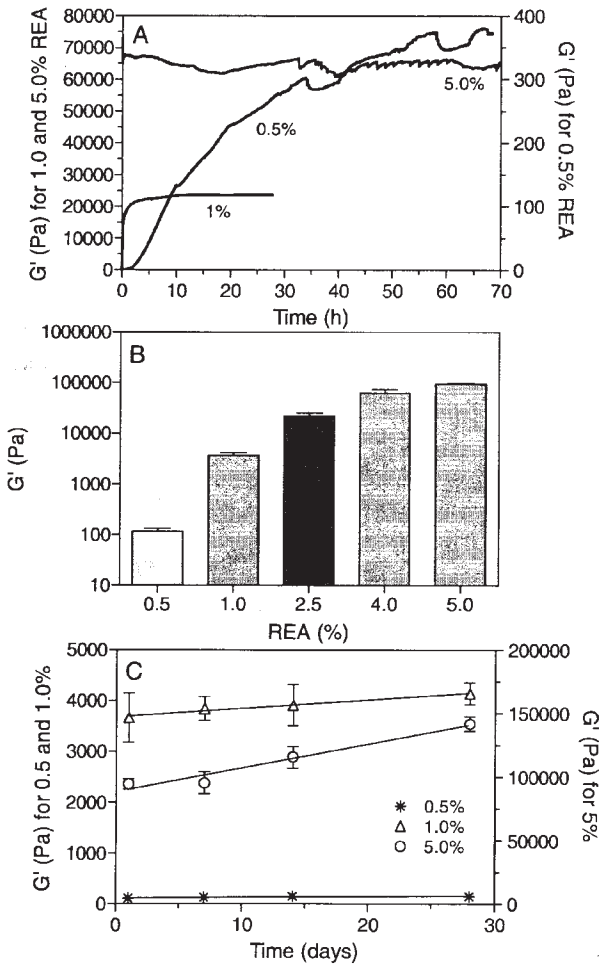

FIG. 1. (A) Changes in storage modulus (G', Pa) of 0.5, 1.0, and 5.0% ricinelaidic acid (REA)–canola oil (CO) blends during gelation at 5°C (0.15% strain, 1 Hz); (B) effect of REA concentration (0.5, 1.0, 2.5, 4.0, and 5.0%) on the 24-h linear viscoelastic region storage modulus (G', Pa) for REA–canola oil gels at 5°C; (C) changes in the linear viscoelastic region storage modulus (G', Pa) for 0.5, 1.0, and 5.0% REA–canola oil gels during storage at 5°C.

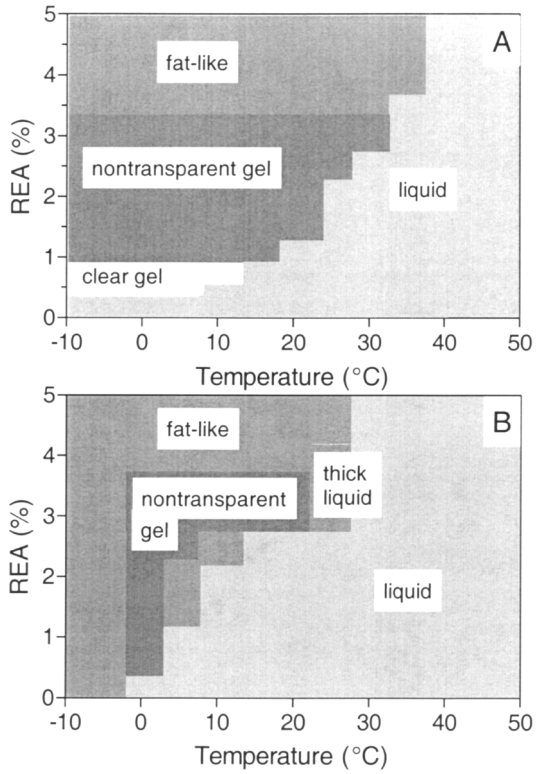

FIG. 2. Phase diagram for REA–CO (A) and REA–sesame oil (B). These phases are described as fat-like (i.e., the material appeared more crystalline than gelled), nontransparent (i.e., self-standing gels ranged from slightly translucent to completely opaque), clear (i.e., self-standing gel was completely transparent), liquid (i.e., no thickening or gelation observed), and thick liquid (i.e., liquid was visibly thickened, but self-standing gel was not observed). For abbreviations see Figure 1.

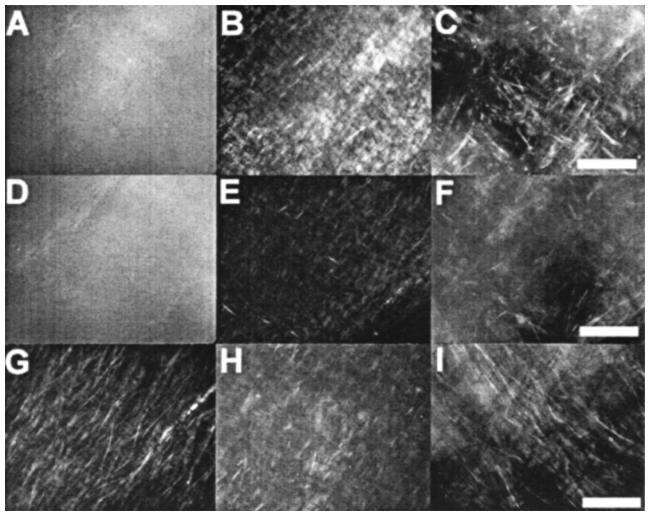

FIG. 3. Partially polarized light micrographs for 0.5% (A, D, G), 1.0% (B, E, H), and 5.0% (C, F, I) REA–CO gels after 1 (A, B, C), 7 (D, E, F) and 28 (G, H, I) days at 5°C. Magnification bars represent 100 μm. For abbreviations see Figure 1.

the potential to participate in hydrogen bonding and therefore impede REA self-assembly. In addition, sterols and tocopherols contain large ring structures that may sterically interfere with the ability of REA to aggregate. A transparent gel was never observed with sesame oil. However, a fifth type of phase was apparent and described; region E refers to samples that were visibly thickened, but not gelled. This behavior represented a transition between the formation of a translucent-opaque gel (region B) and a liquid sample (region D). No such intermediary phases were observed with the CO samples.

The phase behavior was also studied for REA with DAG oil. However, no thickening or gelation was observed after 24 h (data not shown). DAG oil is prepared from CO and soybean oil. It differs from natural seed oils, including CO and sesame oil, in that it is made up of DAG molecules (as the name implies) rather than TAG. In DAG molecules there is a free hydroxyl group on the glycerol backbone, which is otherwise esterified to a FA in the case of TAG. This high number of hydroxyl groups in the DAG oil was correlated with a lack of REA gelation. This lends further evidence to the argument that hydrogen bonding is critical to REA gelation.

Gel structure. When neat REA crystallizes, it forms large spherulites containing needle-like crystals (data not shown). A very different network is observed for the organogels. Polarized light micrographs of the REA gels revealed the presence of long birefringent fibers, which are characteristic of organogels (2). Images of the 0.5, 1.0, and 5.0% REA-CO gels at 5°C after 24 h are shown in Figure 3 (A, B and C, respectively). Figure 3 also shows the gel structure after 7 (Fig. 3D–F) and 28 (Fig. 3G–I) days of storage (see discussion below).

The influence of REA concentration on gel microstructure is very apparent after 24 h. At 0.5% REA (Fig. 3A), the networks were very difficult to visualize. Only when the samples were flooded with light and partially polarized could any struc-

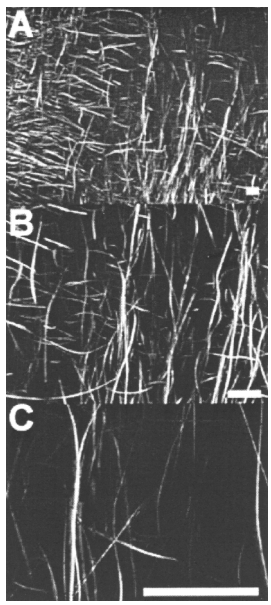

FIG. 4. Polarized light micrographs of 1.5% REA–CO gel at 4, 10, and 40× magnification after 24 h at 20°C. Magnification bars represent 100 μm. For abbreviations see Figure 1.

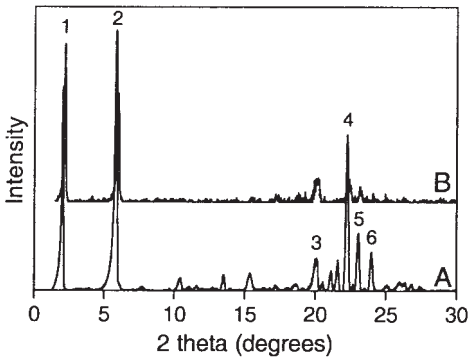

FIG. 5. Powder X-ray diffraction patterns for neat REA (A) and 5.0% REA–CO gel (B) after 24 h at 5°C. Numbers 1–6 refer to spacings for neat REA: 43.28, 15.16, 4.41, 3.99, 3.86, and 3.71Å, respectively.

ture be seen. At higher concentrations (Fig. 3B, C), more of the individual strands were apparent and clusters of the strands were evident. Micrographs for the 20°C 1.5% REA-CO gel at 4, 10, and 40× magnifications are shown in Figure 4. The images demonstrate that some of the fibers exceed ~800 µm in length. Also, Figure 4A shows the edges between two clusters of fibers.

Powder X-ray diffraction (XRD) was used to explore the structure of the REA gels in both the small- and wide-angle regions. The XRD patterns for neat REA and the 5% REA-CO gel after 24 h at 5°C are shown in Figure 5. The peaks identified in Figure 5 correspond to those for neat REA.

The patterns for the neat REA and REA organogels are similar, suggesting a relationship between the molecular packing in the neat and gel phases. Both neat REA and the gel have small-angle reflections that roughly correspond to the 001 and 003 planes. This is similar to neat HSA, which shows characteristically intense (001) and (003) reflections that shift to different extents depending on the solvent.

HSA organogels consist of randomly distributed long fibers, interconnected through junction zones, i.e., monoclinic crystalline domains. The fibers themselves are made up of FA dimers, which form through hydrogen bonding between the hydroxyl groups at C12 and carboxyl groups that are aligned head to head (8). The small-angle reflections observed for the REA gels suggest the presence of dimers and a structure similar to HSA. Crystallinity is evidenced by the presence of the short Bragg spacings. Neither small- nor wide-angle reflections were observed for the 0.5 and 1.0% REA–CO gels after 24 h at 5°C. This is likely related to equipment sensitivity issues at low solids, as gelation was observed and structure was evident by microscopy (Fig. 3A, B).

There is a shift toward slightly higher peak positions in the gel phase (for example, 43.28 Å for neat REA vs. 40.54 Å for the gel). Shifts and peak broadening can occur when liquid molecules are included in the network strands (2). For example, HSA aerogel structures (formed by the evaporation of the organic solvents from organogels) have slightly, but consistently higher values of d-spacings than neat HSA (8). In our case, a shift toward smaller spacings in the REA gels was observed, indicating a different and more closely packed arrangement of the REA dimers within the strands than in the neat crystalline state. The properties of the solvent strongly influence the shape and dimensions of organogelator assemblies (1). These results point to differences between gelator aggregation in organic solvents and in vegetable oil. REA also exhibits polymorphism (data not shown). Differences in REA polymorphic behavior between the neat and gel phases may also explain the differences observed.

Frequency sweeps were performed to probe the nature of the REA gels at 5°C. The results for 0.5, 1.0, 3.0, and 5.0% REA after 24 h are shown in Figure 6.

In all cases, the initial storage modulus (G') was greater than the loss modulus (G''). The 0.5% gel behaved differently from the more concentrated samples. Figure 6A shows that G' was frequency dependent, and a cross-over point was observed for

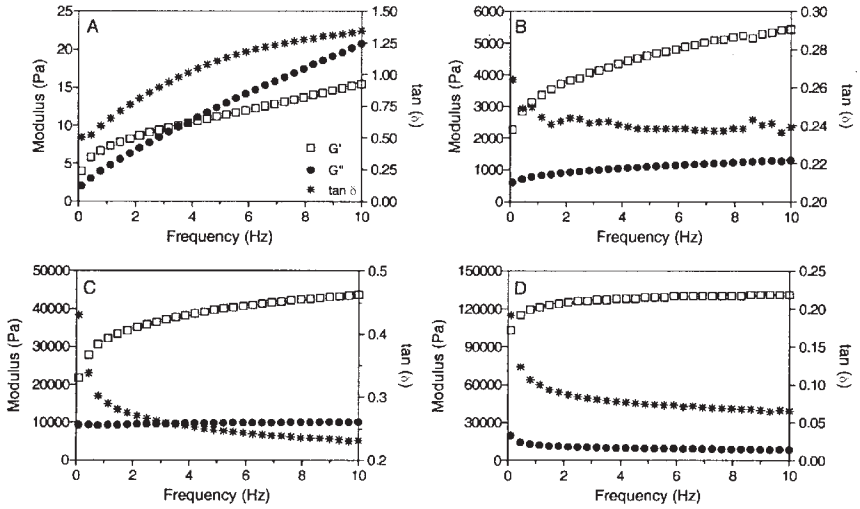

FIG. 6. Storage (G') and loss (G'') moduli and tan δ during frequency sweeps (0.1 to 10 Hz) for 0.5 (A), 1.0 (B), 3.0 (C), and 5.0% (D) REA–CO gels stored at 5°C for 24 h.

TABLE 2
Spacings (Å) Detected by Powder X-Ray Diffraction Spectroscopy for 0.5, 1.0, and 5.0% REA-Canola Oil Blends Stored at 5°C for 1, 7, and 28 d

Days	0.5%	1.0%	5.0%
1	ND[a]	ND	40.5 ± 0.0
			14.8 ± 0.0
			4.4 ± 0.0
			4.0 ± 0.0
			3.9 ± 0.0
			3.8[b]
7	40.8 ± 1.3	41.1 ± 0.8	42.7 ± 0.2
	14.78[b]	14.9 ± 0.1	15.0 ± 0.0
			4.4 ± 0.0
			4.0 ± 0.0
			3.9 ± 0.0
28	41.1 ± 1.0	40.7 ± 1.3	41.7 ± 0.8
	14.9 ± 0.0	14.9 ± 0.1	14.9 ± 0.1
		4.4[b]	4.4 ± 0.0
		4.0[b]	4.0 ± 0.0
			3.9 ± 0.0

[a]ND, no peak detected. For other abbreviation see Table 1.
[b]Indicates spacing was only detected in one replicate. Spacings (Å) for neat REA: 43.28 ± 0.001, 15.16 ± 0.01, 4.41 ± 0.00001, 3.99 ± 0.00001, 3.86 ± 0.001, and 3.71 ± 0.0001.

the 0.5% gel at ~4 Hz. A strong frequency dependence of G', tan δ >1, and a cross-over point where G'' exceeds G' are characteristics of engtangled polymeric solutions (18).

A slight positive slope for G' is consistent with the presence of a weak gel. This was observed for the 5.0% sample (Fig. 6D). The 1.0 and 3.0% gels showed a relatively higher frequency dependence, although tan δ was less than one and no cross-over points were observed for these gels (Fig. 6B–D). These results suggest that, whereas the 0.5% gel consists of entangled fibers, the 1.0, 3.0, and 5.0% gels are stabilized by junction zones between the fibers. This is consistent with the XRD and microscopy data. Very little, if any, birefringence was observed for the 0.5% gels after 24 h (Fig. 4A), and no diffraction peaks were observed in the wide-angle region (refer to Table 2). At higher concentrations, both the light microscopy and XRD analyses indicate the presence of crystallinity, which is expected in the junction zones between REA fibers, i.e., the microcrystalline domains.

Gel stability. Structural and rheological changes in the REA gels stored at 5°C were determined with time. After 7 d of storage, the 0.5% gel changed from a clear to a cloudy gel and the 1.0% sample changed from a cloudy to a more opaque gel. Visible changes were not observed in the 0.25 and 5.0% samples during 28 d of storage; the 0.25% sample remained liquid and the 5.0% appeared "fat-like" throughout the time period. The most significant change in gel microstructure with time was observed for the 0.5% sample between 7 and 28 d (Fig. 3D vs. Fig. 3G). After 28 d, an increase in the number and thickness of fibers was evident in the 0.5% sample. The 0.5, 1.0, and 5.0% gels had similar networks as visualized by microscopy after 28 d, although the gels differed substantially in terms of their visual appearance; the 0.5, 1.0, and 5.0% gels appeared as a cloudy gel, an opaque gel, and fat-like, respectively. Changes in the G' and XRD patterns during storage at 5°C are shown in Figure 1C and Table 2, respectively.

Significant increases in G' were observed for the 1.0 and 5.0% samples in time ($P < 0.05$), although not for the 0.5% gels ($P = 0.16$). These results indicate continued setting and/or restructuring of the gels. The observed increases in gel opacity and changes in microstructure of the 0.5% sample also indicate the dynamic nature of the gels. Similarly, Table 2 shows that changes were observed in the scattering properties of the gels during storage. After 1 d, no x-ray scattering was observed for the 0.5 and 1.0% gels. However, after 7 d, peaks in the small-angle region were detected, suggesting the presence of more REA dimers. In addition, wider-angle reflections were detected in the 1.0% gel after 28 d. Although more order was observed for the dilute gels, there were no significant trends in the XRD patterns for the 5.0% gels during storage ($P > 0.05$). The positions of the ~41 and ~15 Å peaks neither increased nor decreased over time for the 5.0% gel. Similarly, the interplanar spacings were not significantly different for the three concentrations studied after 28 d ($P > 0.05$). Overall, these results indicate continual reorganization of the REA gels at 5°C, leading to an increase in the microcrystalline domains. This reorganization may be likened to retrogradation in polysaccharide gels.

ACKNOWLEDGMENTS

This work was funded, in part, by the Natural Sciences and Engineering Research Council of Canada and the Ontario Ministry of Agriculture, Food and Rural Affairs.

REFERENCES

1. Abdallah, A.J., and R.G. Weiss, Organogels and Low Molecular Mass Organic Gelators, *Adv. Mater. 12*:1237–1247 (2000).
2. Terech, P., and R.G. Weiss, Low Molecular Mass Gelators of Organic Liquids and the Properties of Their Gels, *Chem. Rev.* 97:3133–3159 (1997).
3. Van Esch, J.H., and B.L. Feringa, New Functional Materials Based on Self-Assembling Organogels: From Serendipity Towards Design, *Angew. Chem. Int. Ed. 39*:22636–22666 (2000).
4. Scartazzini, R., and P.L. Luisi, Organogels from Lecithin, *J. Phys. Chem. 92*:829–833 (1988).
5. Markovic, N.. M. Ginic-Markovic, and N.K. Dutta, Mechanism of Solvent Entrapment Within the Network Scaffolding in Organogels: Thermodynamic and Kinetic Investigations, *Polym. Int. 52*:1095–1107 (2003).
6. Mukkamala, R., and R.G. Weiss, Physical Gelation of Organic Fluids by Anthraquinone-Steroid Based Molecules. Structural Features Influencing the Properties of Gels, *Langmuir 12*:1474–1482 (1996).
7. Uzu, Y., Phase Behavior and Colloidal Structure of Lithium Stearate in Hydrocarbons, *J. Jpn. Oil Chem. Soc. 24*:261 (1975).
8. Terech, P., V. Rodriguez, J.D. Barnes, and G.B. McKenna, Organogels and Aerogels of Racemic and Chiral 12-Hydroxyoctadecenoic Acid, *Langmuir 10*:3406–3418 (1994).
9. Hanabusa, K., R. Tanaka, M. Suzuki, M. Kimura, and H. Shirai, Excellent Gelators for Organic Fluids: Simple Bolaform Amides Derived from Amino Acids, *Adv. Mater. 9*:1095–1097 (1997).
10. Okabe, S., K. Ando, K. Hanabusa, and M. Shibayama, Dynamic Light Scattering and Small-Angle Neutron Scattering Studies on Organogels Formed with a Gelator, *J. Polym. Sci. B–Polym. Phys. 42*:1841–1848 (2004).

11. Friggeri, A., O. Gronwald, K. van Bommel, S. Shinkai, and D.N. Reinhoudt, Charge-Transfer Phenomena in Novel, Dual-Component Sugar-Based Organogels, *J. Am. Chem. Soc. 124*:10754–10758 (2002).
12. Terech, P., C. Chachaty, J. Gaillard, and A.M. Godquin-Giroud, Electron Paramagnetic Resonance Study of the Physical Gelation of a Copper Complex in Cyclohexane, *J. Phys. (Paris) 48*:663 (1987).
13. Terech, P., V. Schaffhauser, P. Maldivi, and J.M. Guenet, Living Polymers in Organic Solvents, *Langmuir 8*:2104–2106 (1992).
14. Terech, P., D. Pasquier, V. Bordas, and C. Rossat, Rheological Properties and Structural Correlations in Molecular Organogels, *Langmuir 16*:4485–4494 (2000).
15. Gandolfo, F.G., B. Arjen, and E. Flöter, Structuring of Edible Oils by Long-Chain FA, Fatty Alcohols, and Their Mixtures, *J. Am. Oil Chem. Soc. 81*:1–6 (2004).
16. Marton, L., J.W. McBain, and R.D. Vold, An Electron Microscope Study of Curd Fibers of Sodium Laurate, *J. Am. Chem. Soc. 63*:1990–1993 (1941).
17. AOCS, *Official Methods and Recommended Practices of the AOCS, Section 1: Physical and chemical characteristics of oils, fats and waxes,* AOCS Press, Champaign, IL, 1996, p. 44.
18. Tosh, S.M., P.J. Wood, Q. Wang, and J. Weisz, Structural Characteristics and Rheological Properties of Partially Hydrolyzed Oat β-Glucan: The Effects of Molecular Weight and Hydrolysis Method, *Carb.Polym. 55*:425–436 (2004).

[Received November 28, 2005; accepted March 10, 2006]